rate G consistent with the incident photon flux is 2×10^{23} electrons/cm^2 sec. For this value to yield the measured maximum injected $\bar{N}L$ of $\approx10^{14}$ electrons/cm^2 shown in Fig. 2 we must take the carrier lifetime to be $\tau\approx0.5$ nsec. Diffusion lengths under the high-intensity conditions of this experiment have not been measured, but estimating[10] this length to be ~1 μm yields a maximum electron density $\sim10^{18}$ cm^{-3} for all samples measured.

In conclusion, we have obtained a reliable measure for the total number of electrons injected in GaAs under intense optical excitation. This measurement is independent of any assumption concerning the unknown spatial distribution of the carriers. Further, we have been able to deduce effective carrier lifetimes. All these results demonstrate that even at high excitation levels a significant fraction of the injected carriers can relax to the band edge, where they live long enough to diffuse into the bulk of the crystal.

We thank C. H. Henry for a critical reading of the manuscript. We also thank J. C. DeWinter for growing some of the epitaxial layers and A. L. Albert for sample preparation.

[1]K. L. Skaklee *et al.*, Appl. Phys. Lett. **19**, 302 (1971); J. F. Figueira and H. Mahr, Solid State Commun. **9**, 679 (1971); I. Kh. Akopyan *et al.*, Zh. Eksp. Teor. Fiz. Pis'ma Red. **12**, 366 (19701) [JETP Lett. **12**, 251 (1970)].

[2]G. N. Galkin, L. M. Blinov, V. S. Vavilov, and A. G. Golovashkin, Zh. Eksp. Teor. Fiz. Pis'ma Red. **7**, 93 (1968) [JETP Lett. 7, 69 (1968)].

[3]I. F. Vakhnenko and V. L. Strizhevskii, Sov. Phys.-Semicond. 3, 1562 (1970).

[4]P. D. Dapkus, N. Holonyak, Jr., R. D. Burnham, D. L. Keune, J. W. Burd, K. L. Lawley, and R. E. Walline, J. Appl. Phys. **41**, 4194 (1970).

[5]J. D. Cuthbert, J. Appl. Phys. **42**, 739 (1971).

[6]C. J. Johnson, G. H. Sherman, and R. Weil, Appl. Opt. **8**, 1667 (1969).

[7]M. Born and E. Wolf, *Principles of Optics*, 4th ed. (Pergamon, London, 1970), p. 55.

[8]O. Madelung, *Physics of III-V Compounds* (Wiley, New York, 1964), p. 140.

[9]The possibility exists that ω_0 may also be carrier-density dependent, in which case the intensity-dependent factors contributing to the reflection are $\bar{N}L/\omega_0$. Taking $\bar{N}\sim G\tau/L$, where G is the generation rate per unit cross sectional area and τ is the free-carrrier lifetime, then for $G\propto I$ we conclude that $\tau/\omega_0\propto I^{-0.3}$.

[10]H. C. Casey, Jr., B. I. Miller, and E. Pinkus, J. Appl. Phys. (to be published); C. J. Hwang, Phys. Rev. B **6**, 1355 (1972). These authors have obtained minority-hole diffusion lengths for low-level photoinjection in n-type epitaxial GaAs doped in the range 10^{17}–10^{18} electrons/cm^{-3} and find $L\sim1$ μm.

PHYSICAL REVIEW B VOLUME 8, NUMBER 2 15 JULY 1973

Theory of Electron Micrographs of Amorphous Materials

W. Cochran*

IBM Watson Research Center, Yorktown Heights, New York 10598

(Received 20 November 1972)

A method is given for calculating the electron micrographs of amorphous materials. It is based on the kinematical theory of diffraction and should be valid for specimens of amorphous silicon, for example, up to 100 Å in thickness. It is found that the random-network model for amorphous silicon accounts qualitatively for much of what is observed in electron micrographs obtained experimentally, but features of results obtained by Rudee and Howie using the off-set bright-field configuration appear to require the presence of at least a small proportion of crystallites. More conclusive experimental results could be obtained by using thinner specimens.

I. INTRODUCTION

It is a surprise to a newcomer to the field to find that there is still scope for debate about the structures of certain amorphous materials. The random-network model[1–4] for amorphous germanium and silicon appeared to be gaining general acceptance but has recently been opposed by Rudee and Howie[5] who presented evidence from electron microscopy which they interpreted in terms of a microcrystallite model. Chaudhari *et al.*, who have obtained similar electron micrographs,[6] claim that the observations are not inconsistent with a random-network model.[7] In this paper we put forward a general method, based on the kinematical theory of electron diffraction,[8] for calculating the electron micrographs of amorphous materials, and present some preliminary calculations for silicon. While it is concluded that the random-network model can account for much of what is observed, the experimental evidence is not conclusive, but could be made more so by the use of specimens somewhat thinner than is current practice.

II. KINEMATICAL DIFFRACTION THEORY FOR AMORPHOUS MATERIAL

The kinematical approximation is valid only when the amplitude of a diffracted wave is very

small compared with the incident-wave amplitude, which we take to be unity. Let $\vec{S}$ be the scattering vector, so that $S = (2\sin\theta)/\lambda$ and $f(S)$ is the atomic scattering factor for electrons. Using the kinematical approximation, the scattering cross section per atom in amorphous silicon is

$$\sigma = 2\pi\lambda^2 \int S f^2(S)\, dS + \lambda^2 \int \mathcal{F}(S)\, f^2(S)\, dS. \qquad (1)$$

$\mathcal{F}(S)$ is the "reduced-intensity function" defined for example by Moss and Graczyk[1] and measured experimentally by them for amorphous silicon. Evaluation using data appropriate to silicon, with $\lambda = 0.037$ Å, gives $\sigma = 2.43\times10^{-2}$ Å^2. The second term in Eq. (1) contributes only about -16%; the first term gives the intensity appropriate to atoms in random positions, without preferred interatomic distances. The intensity scattering out of a specimen of thickness t is therefore $\sigma t/v$, where v is the atomic volume. For a specimen of thickness 33 Å this is 3.75×10^{-2}, so that 96.2% of the intensity remains in the direct beam. The kinematical approximation should therefore be valid for thicknesses of amorphous silicon of this order of magnitude. (We also note that approximately 95% of the scattered intensity is within $2\theta = 5°$ of the direct beam.)

Two experimental configurations were used by Rudee and Howie. In the first the direct beam and a segment of the diffraction pattern were allowed through the objective aperture. This is illustrated in Fig. 1, where O is the position of the direct beam (the origin in reciprocal space), and the heavy line is a segment of the first maximum of the diffraction pattern, which for silicon occurs at $S = 0.32$ Å^{-1}. The aperture defines a limiting circle in reciprocal space of radius $S_0 = 0.34_5$ Å^{-1}, and the center of this circle is at a distance $S_{cx} = 0.19_1$ Å^{-1} from O. The center of the aperture was assumed to coincide with the axis of the instrument. With the wavelength used, it is an excellent approximation to take the Ewald sphere to be a plane over the area defined by the circle of radius S_0. The normal to the plane which is a closest approximation is inclined to the direct beam at an angle somewhat less than λS_{cx}. Numerically λS_{cx} is 0.4°, so that for all practical purposes the image formed in the microscope must correspond to a projection of the specimen on a plane perpendicular to the direct beam. In the second experimental configuration, which gives a dark-field image, S_{cx} was 0.44 Å^{-1} so that the direct beam was intercepted. (Rudee and Howie experimented with germanium, we have scaled the dimensions to be appropriate to silicon.)

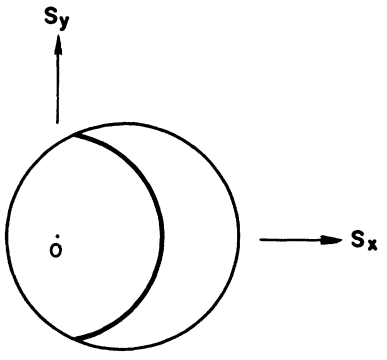

FIG. 1. Position of the direct beam O and a segment of the first diffraction maximum in relation to the aperture, for the off-set bright-field configuration.

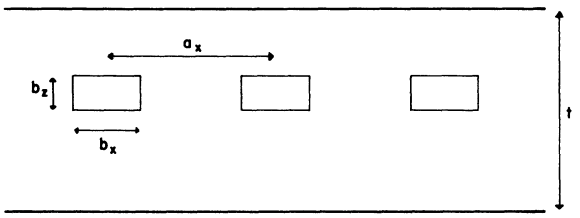

FIG. 2. Specimen of thickness t is imagined to be composed of structureless material with a constant potential, and of blocks containing atoms.

The next step was suggested by the work of Henderson and Herman[2] in that periodic boundary conditions are imposed in specifying the structure of the amorphous material. In this way the problem is converted into one involving a "perfect crystal" as specimen. No serious error or approximation is involved however since the unit cell can be made arbitrarily large. In Fig. 2, the specimen of thickness t is taken first of all to be a completely smeared-out distribution of atoms giving a constant potential inside the specimen. Electrons are not then scattered, but the phase of the direct beam is retarded by the correct amount, to correspond to the refractive index. A "block" of this material measuring b_x, b_y, b_z is now imagined to be removed and replaced by a block of perfect crystal, or by a block representative of the random-network model, or any other model. These blocks are repeated indefinitely with spacing a_x, a_y in two dimensions to give a unit cell of volume $a_x a_y b_z$ which thus consists partly of material with a specified atomic structure and partly of smeared-out material. The smeared-out material above and below the two-dimensional array can be ignored since it merely retards equally the phases of the direct and diffracted beams. The material between the blocks could be eliminated by making $a_x = b_x$ and $a_y = b_y$ but we shall see that it is advantageous not to do so immediately. The allowed values of the scattering vector are now given by

$$\vec{S} = \vec{H}, \qquad (2)$$

where $\vec{H}$ is a vector in the two-dimensional reciprocal lattice, for which the spacings are a_x^{-1} and a_y^{-1}. (It is more convenient to exclude the customary factors of 2π.) The structure factor of the "crystal" which we have constructed in this way is

$$F(\vec{H}) = f(H)\left(\sum_{j=1}^{N} e^{2\pi i \vec{H}\cdot\vec{r}_j} - N\,\frac{\sin\pi b_x H_x}{\pi b_x H_x}\,\frac{\sin\pi b_y H_y}{\pi b_y H_y}\right). \tag{3}$$

There are N atoms in a block, $\vec{r}_j$ is an atomic coordinate (the z coordinate is irrelevant, as explained earlier), and the second term takes account of the smeared-out material removed from each block. The origin is at the center of a block.

The amplitude of each diffracted beam is now given by

$$i\lambda b_z F(\vec{H})/V = i\lambda F(\vec{H})/A \tag{4}$$

(see, for example, Hirsch *et al.*[8]) where $V = a_x a_y b_z$ is the volume of the unit cell and A is its area in projection. In what follows we take $a_x = a_y = a$ so that $A = a^2$. It is now easily shown, following the discussion of the situation which involves the direct beam and one diffracted beam,[8] that for the first experimental configuration the intensity at a point $\vec{r}$ in the image is given by

$$I(\vec{r}) = |\psi(\vec{r})|^2 = \left|1 + i\,\frac{\lambda}{A}\sum{}' F(H)\, e^{-2\pi i \vec{H}\cdot\vec{r}}\right|^2. \tag{5}$$

For the second experimental configuration the intensity is

$$\tilde{I}(\vec{r}) = \left(\frac{\lambda}{A}\right)^2 \left|\sum{}' F(\vec{H})\, e^{-2\pi i \vec{H}\cdot\vec{r}}\right|^2. \tag{6}$$

In each instance the sum $\sum'$ is over the points of the reciprocal lattice which fall inside the circle of radius S_0 and center S_{cx}. Now writing

$$F(\vec{H}) = |F(\vec{H})|\, e^{i\phi(\vec{H})} \tag{7}$$

and defining

$$C_1(\vec{r}) = \frac{2\lambda}{A}\sum{}' |F(\vec{H})| \sin[2\pi\vec{H}\cdot\vec{r} - \phi(\vec{H})], \tag{8}$$

$$C_2(\vec{r}) = \frac{2\lambda}{A}\sum{}' |F(\vec{H})| \cos[2\pi\vec{H}\cdot\vec{r} - \phi(\vec{H})], \tag{9}$$

it is found that Eq. (5) reduces to

$$I(\vec{r}) = 1 + C_1(\vec{r}) + \tfrac{1}{4}[C_1^2(\vec{r}) + C_2^2(\vec{r})] \tag{10}$$

(off-set bright-field configuration), while Eq. (6) reduces to

$$\tilde{I}(\vec{r}) = \tfrac{1}{4}[C_1^2(\vec{r}) + C_2^2(\vec{r})] \tag{11}$$

(dark-field configuration).

Equation (10) is much the more interesting of the two. For the thickness b_z with which we shall be concerned $C_1(\vec{r})$ is small compared with unity, typically < 0.3, and the term $\frac{1}{4}[C_1^2(\vec{r}) + C_2^2(\vec{r})]$ can be neglected. (It is of the same order of magnitude as an error already introduced by taking the amplitude of the transmitted direct beam to be unity, and partly cancels this.) We therefore have for the contrast in the off-set bright-field micrograph,

$$C_1(\vec{r}) = \frac{I(\vec{r}) - \langle I(\vec{r})\rangle}{\langle I(\vec{r})\rangle} = \frac{2\lambda}{A}\sum{}' |F(\vec{H})| \sin[2\pi\vec{H}\cdot\vec{r} - \phi(\vec{H})]. \tag{12}$$

The interesting feature of this result is that it involves the structure factors *linearly*. We also find later that the intensity or contrast originating in a particular block, of area about 10×10 Å, "spills out" very little from the corresponding area in the image. Thus the linear dependence on structure factor enables us to superpose the contributions originating from different areas of a specimen, two representative blocks placed side by side do not produce overlapping images until they are quite close, but if placed one behind the other the intensities which each contributes simply add. Thus we can imagine the specimen of thickness t to be built up by adding blocks, all different from one another, until the smeared-out material is eliminated. These results do not apply to the dark-field image. Blocks which are sufficiently separated laterally do contribute independently, but those separated only in the z direction do not. We must then take $b_z = t$.

III. NUMERICAL CALCULATIONS FOR SILICON

These were made first of all for a block of silicon having the diamond structure, with (111) on the S_x axis and $(2\bar{2}0)$ on the S_y axis. Its dimensions were $9.4\times9.6\times13.45$ Å, with $N = 60$, and thus three (111) planes in the x direction. The computed contrast, using Eq. (12), is shown in Fig. 3(a) for $y = 0$, that is along a line passing through the center of the crystallite. The result shown was obtained with $a_x = a_y = 40$ Å, but since the function falls practically to zero for $x > 6$ Å all that is necessary is that a_x and a_y should exceed about 20 Å. The intensity is constant in the y direction until the edge of the block is approached, falling to zero beyond about $y = 6$ Å. The amplitude of the fringes is close to the value 0.133 which is that appropriate to a crystal of indefinite extent in the xy plane, and thickness 13.45 Å.

Spherical aberration is the most important lens aberration in an electron microscope. The phase shift of a beam inclined at an angle α to the axis of the instrument is[8]

$$\epsilon = 2\pi\left(\frac{C_s\alpha^4}{4\lambda} - \frac{\Delta\alpha^2}{2\lambda}\right), \tag{13}$$

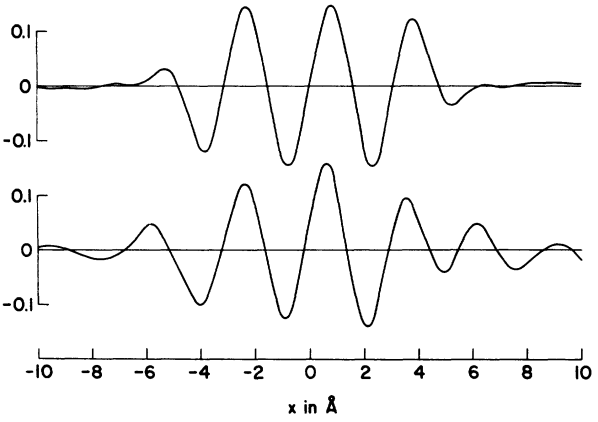

FIG. 3. Contrast produced in the off-set bright-field configuration by a crystallite (a) in a perfect microscope, (b) with allowance for spherical aberration and defocusing.

where C_s is the spherical-aberration constant. The effect of underfocusing the objective lens by an amount Δ is also included in Eq. (13), and this may be used to minimize the effect of spherical aberration. This phase shift results in the replacement of $\phi(\vec{H})$ by $\phi(\vec{H})+\epsilon(\vec{H})-\epsilon(0)$ in the bright-field configuration, and of $\phi(\vec{H})$ by $\phi(\vec{H})+\epsilon(\vec{H})$ in the dark-field configuration.

The calculation described in the first paragraph was repeated with $C_s = 1.6$ mm and $\Delta = 4.7\times10^{-6}$ cm; the result is shown in Fig. 3(b). The fringes remain quite recognizable but ripples now spread further into the area surrounding each block.

To represent a block of silicon with the random-network structure we took a 61-atom structure generated by the computer program of Henderson and Herman.[2] The volume of the block was taken to be $(10.85)^3$ Å^3, 10.85 Å being twice the dimension of the cubic unit cell of crystalline silicon. We are thus taking the relative density of amorphous silicon to be $\frac{61}{64}$, a reasonable value.[9] The Henderson–Herman structure satisfies periodic boundary conditions but we have not made use of this fact. We use XYZ to denote directions in this structure. Figure 4 shows the computed contrast for $x=X$, $y=Z$ (the choice will be explained later). The contours are at ±0.05, 0.10, 0.15, and the block is outlined (ignore the diagonally drawn lines meantime). The contrast falls practically to zero within 1–2 Å of the boundary. Inclusion of the phase shifts ϵ did not produce an essential alteration of the pattern. To simulate a thicker specimen without the mental effort of imagining several such contour maps superposed we piled the 61-atom structure on top of itself so that the xy projection was a superposition of the XY, ZX, and YZ projections, giving a thickness of 32.6 Å. The computed contrast is shown in Fig. 5. The maximum contrast is now about 0.25, the mean-square contrast is three times greater than in Fig. 4. The number of maxima is about the same in both.

These calculations were repeated for the dark-field configuration, using Eq. (11). The position of the aperture was as given in Sec. II. It should be remembered that we now have to consider the

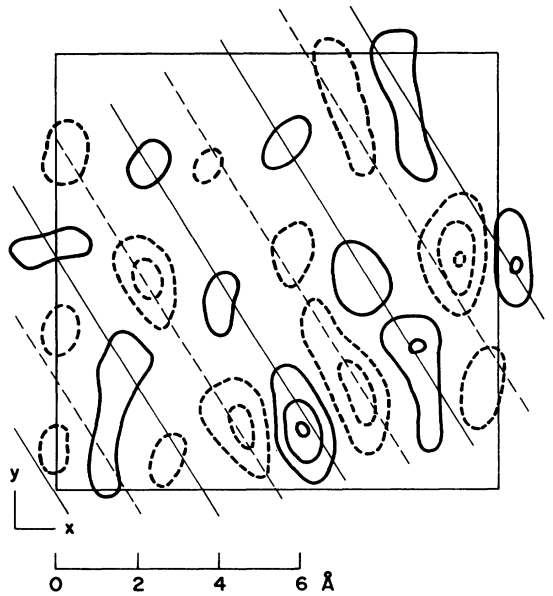

FIG. 4. Contrast produced by a block of material 10.85 Å thick having a random-network structure. Contours are drawn at ±0.05 to ±0.15 with interval 0.05. The unbroken diagonal lines have a spacing of 3.13 Å.

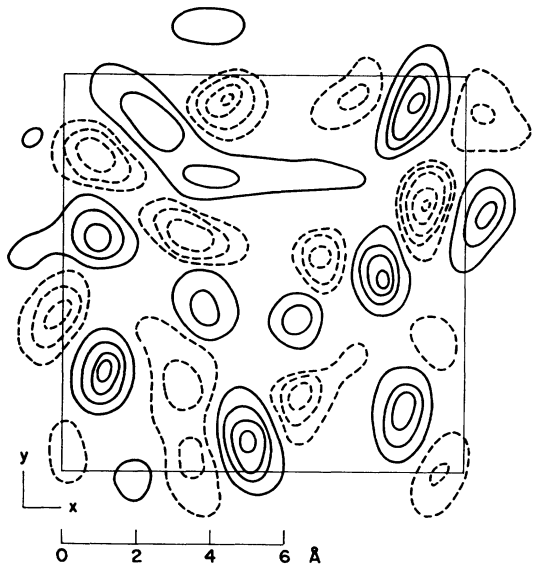

FIG. 5. Contrast produced by a block of material 32.6 Å thick having a random-network structure. Contours are drawn at ±0.05 to ±0.25 with interval 0.05.

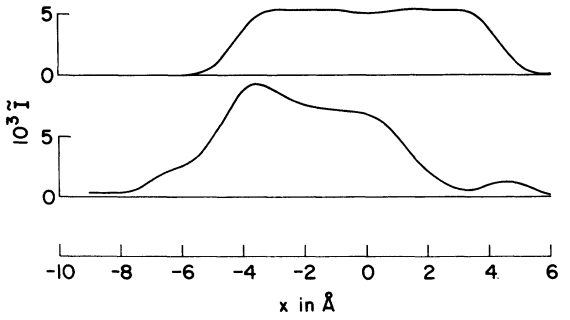

FIG. 6. Intensity produced in the dark-field configuration by a crystallite (a) is a perfect microscope. (b) with allowance for spherical aberration and defocusing.

thickness t of the specimen to be equal to b_g [unless the material behind and in front of the block we are considering is highly crystalline, and not oriented so as to give a (111) reflection].

Figure 6 shows the computed intensity in the image of a crystallite of the same dimensions as before, without and with allowance for instrumental effects [Eq. (13)]. Particularly in the former instance, the intensity spreads little outside the boundaries of the block. Figure 7 shows the computed intensity for the 32.6-Å thickness of random-network structure. The contours are at 5, 10, and 15×10^{-3}. It should be recalled that the scale is such that the intensity in the absence of a specimen would be unity in the bright-field configuration.

As a check on the internal consistency of these calculations, the intensity in the dark-field image was calculated for $S_0 = 1.3$ Å^{-1} and $S_{cx} = 0$ (a configuration that could not be achieved in practice). The average intensity in the image $\langle\tilde{I}\rangle$ was found to be 2.76×10^{-2}. Making an estimated correction of +19% for the contribution still cutoff by the aperture raises this to 3.25×10^{-2}, in reasonable agreement with the estimate of the fraction of the intensity diffracted, made in Sec. II for material of this thickness.

IV. DISCUSSION

The intensity in the image for the dark-field configuration, shown in Fig. 7, and in other maps which have been calculated but are not shown, has all the features of the micrographs which are obtained experimentally,[5,6] as far as can be determined by examination of the published photographs. The off-set bright-field configuration, however, provides a more critical test. The contrast shown in Figs. 4 and 5 resembles qualitatively much of what can be seen in the photograph published by Rudee and Howie; a pattern of bright and dark "blobs," each bright blob having typically some four or so nearest neighbors at distances between 3 and 4 Å. This distance, incidentally, is more a feature of the position of the aperture than of the random-network model; a random model in which there are no preferred interatomic distances does not give a very different computed contrast in its general features. There are however in the photograph regions where the bright blobs line up to give the appearance of a "string of beads," and there are just a few places where as many as four bright fringes can be seen, somewhat broken in the direction perpendicular to the wave vector and not extending further than 6 Å in this transverse direction. It is highly improbable that the random-network model can account for this feature. Let us return to a consideration of Fig. 4, which shows the contrast arising from a block of random-network structure of thickness 10.85 Å. This projection was chosen for illustration because a structure factor for which H is very close to 0.32 Å^{-1}, the reciprocal of $d(111)$, is unusually large, almost half the value appropriate to a diamond-type crystallite of the same volume.[7] Yet no fringes are to be seen in Fig. 4. However when the crests (continuous lines) and troughs (dotted lines) of a wave of wavelength $d(111) = 3.13$ Å are drawn in, as in Fig. 4, it is apparent that most positive peaks fall on crests, and most negative peaks in troughs. For a block of random-network structure to produce recognizable fringes covering an area A', *one* of the "essentially independent" structure factors, of which the number is[10] $\pi S_0^2 A'$, must be large, *and* the remainder must be small, or the fringes will be broken up and become unrecognizable. One can estimate that the fringes will be recognizable only

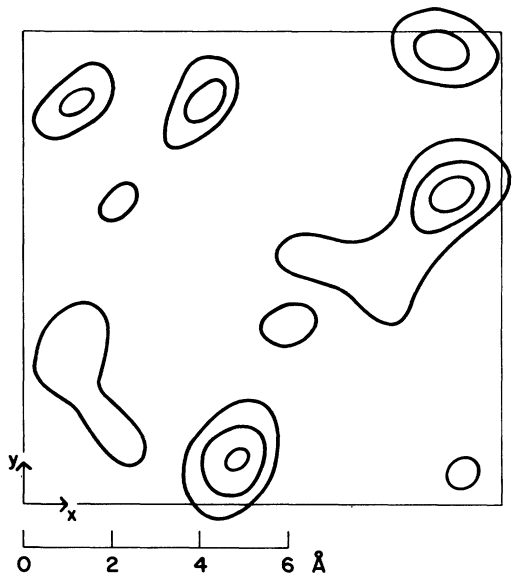

FIG. 7. Intensity produced by a block of material 32.6 Å thick having a random-network structure. Contours are drawn at 5, 10, and 15×10^{-3}.

when their amplitude, produced by one structure factor, is at least as large as the root-mean-square contrast produced by all other structure factors. The probability of this occurrence has been estimated using the theory of the statistics of structure factors[11]; to give the calculation here in full would be too great a digression, suffice to say that for any reasonable area of fringes and thickness of specimen the probability is extremely small. (See Appendix.)

Conversely, let us suppose that a block of crystallite in the correct orientation has produced a few fringes of amplitude 0.14, as in Fig. 3. For these to be recognizable, any material in a random-network, or simply random, array which fills the space between randomly oriented crystallites, and which comes behind or in front of the crystallite producing fringes, must give a root-mean-square contrast less than about 0.14. Consideration of the experiment of Rudee and Howie, where the specimen had a thickness of 200 Å, suggests that the necessary condition could seldom be satisfied. More conclusive results could be obtained by using thinner specimens, which would have the added advantage of making possible a quantitative comparison of theory and experiment. We estimate that the theory given here will give reasonably satisfactory results for specimens of silicon up to 100 Å thick, subject to some obvious conditions such as the absence of crystallites of comparable dimensions of course.[12]

ACKNOWLEDGMENTS

I am grateful to several colleagues, particularly Dr. P. Chaudhari and Professor J. Silcox, for helpful discussions.

APPENDIX

It was shown by Wilson[11] that the probability distribution for $|F|^2$ is

$$P(|F|^2)d|F|^2 = \frac{d|F|^2}{\langle|F|^2\rangle}\exp\left(-\frac{|F|^2}{\langle|F|^2\rangle}\right), \quad \text{(A1)}$$

where $\langle|F|^2\rangle$ is the average value, appropriate to the range of $S=(2\sin\theta)/\lambda$ under consideration. It follows that the probability that $|F|$ exceeds some specified value $|F_1|$ is

$$P(|F|>|F_1|)=\exp(-|F_1|^2/\langle|F|^2\rangle). \quad \text{(A2)}$$

Suppose fringes are to be formed covering an area A'. The number of atoms above this area of a specimen of thickness t, which contribute to F, is

$$N=A't/v, \quad \text{(A3)}$$

where v as before is the atomic volume. A pattern confined to an area A' requires

$$m=\pi S_0^2 A'. \quad \text{(A4)}$$

Fourier coefficients in order to define it,[10] where πS_0^2 is the area in reciprocal space from which the coefficients are drawn. The m points are to be taken to be distributed on a lattice with a unit-cell area $(A')^{-1}$ in reciprocal space. To form fringes of maximum contrast C_1 or greater we require a structure factor of magnitude at least

$$|F_1| = A' C_1/2\lambda \quad \text{(A5)}$$

[see Eq. (8)]. The value of S appropriate to this structure factor must be acceptably close to 0.32 to give fringes of the correct spacing [$d(111)=3.13$ Å for silicon]. The remaining $(m-1)$ structure factors are to give a "random" contrast of root-mean-square value not exceeding C_1. We take the condition to be that each such structure factor must not exceed $F_1/(m-1)^{1/2}$.

To illustrate the principle of the calculation we can take the atomic coordinates to be random so that

$$\langle|F|^2\rangle = Nf^2 \quad \text{(A6)}$$

and also ignore the variation of f^2 across the aperture. The probability that one structure factor is adequately large and all others are adequately small is now

$$p' = \exp\left(-\frac{|F_1|^2}{\langle|F|^2\rangle}\right)\left[1-\exp\left(\frac{-|F_1|^2}{(m-1)\langle|F|^2\rangle}\right)\right]^{m-1}. \quad \text{(A7)}$$

However, of the m points it is estimated that

$$n \approx \pi(A')^{1/2}/d(111) \quad \text{(A8)}$$

of them will have a value of S acceptably close to $1/d(111)$. The probability of "recognizable" fringes covering an area A' with contrast greater than C_1 is thus approximately

$$p = np' \quad \text{(A9)}$$

when the atoms in the specimen are distributed at random.

It is estimated that an area of at least 40 Å^2 is required to define fringes of measurable spacing. Substituting values appropriate to silicon, with $S_0=0.34$ Å^{-1} and $C_1=0.2$, one finds that p as a function of t does not vary greatly between $t=20$ and 100 Å, the maximum value being 8.3×10^{-8} at $t \approx 40$ Å.

A better calculation takes account of the variation of $\langle|F|^2\rangle$ with S, and thus of the radial distribution of the atoms, and of the fact that any two structure factors at $+\vec{S}$ and $-\vec{S}$ cancel from the Fourier series for C_1. The maximum value of p is then increased to 8.9×10^{-6} at $t\approx 50$ Å. This, while small, is not negligible. However p decreases rapidly with increasing A'. In the published micrograph[5] a "degree of regularity" in the

contrast, covering as much as 100 Å^2, can sometimes be seen; the pattern is such as could result from fringes produced by a crystallite, with a superposed random contrast from another part of the specimen, behind or in front of the crystallite. Considerations set out above make this a much more likely explanation than that the fairly regular pattern observed could all originate from a volume $A't$ of material with a random-network structure.

*Summer visitor from University of Edinburgh, United Kingdom.
[1]S. C. Moss and J. F. Graczyk, Phys. Rev. Lett. **23**, 1167 (1969).
[2]D. Henderson and F. Herman, J. Non-Cryst. Solids **8**, 359 (1972).
[3]N. J. Shevchik, Bull. Am. Phys. Soc. **16**, 347 (1972).
[4]D. E. Polk, J. Non-Cryst. Solids **5**, 365 (1971).
[5]M. L. Rudee and A. Howie, Philos. Mag. **25**, 1001 (1972).
[6]P. Chaudhari, J. F. Graczyk, and S. R. Herd, Phys. Status Solidi B **51**, 801 (1972).
[7]P. Chaudhari, J. F. Graczyk, and H. P. Charbnau, Phys. Rev. Lett. 29, 425 (1972).
[8]P. B. Hirsch, A. Howie, R. B. Nicholson, D. W. Pashley, and M. J. Whelan, *Electron Microscopy of Thin Crystals* (Plenum, New York, 1965).
[9]M. H. Brodsky, D. Kaplan, and J. F. Ziegler, Appl. Phys. Lett. 21, 305 (1972).
[10]A. Klug and R. A. Crowther, Nature (Lond.) **238**, 435 (1972).
[11]A. J. C. Wilson, Acta Crystallogr. **2**, 318 (1949).
[12]Since my return to Edinburgh, I learned that similar calculations have been made for SiO_2 by A. Howie, O. Krivanek, and M. Rudee [Philos. Mag. 27, 235 (1973)]. We agree in our general conclusions.

PHYSICAL REVIEW B VOLUME 8, NUMBER 2 15 JULY 1973

Interaction of Acoustic Waves with Acceptor Holes in Silicon: The Influence of Internal Stress

Takehiko Ishiguro
Electrotechnical Laboratory, Mukodai, Tanashi, Tokyo 188, Japan
(Received 22 January 1973)

The temperature and the magnetic field dependences of the ultrasonic attenuation are measured at low temperatures in lightly doped p-Si samples with various impurity concentrations and dislocation densities. In the dislocation-free sample, a peak is found in the temperature dependence, which is related to the content of acceptors. In the sample with high dislocation density (2×10^4 cm^{-2}), an additional attenuation is found below 3 K which is ascribed to the resonance absorption by acceptor holes and the attenuation is quenched with a lower magnetic field (about 10 kG) than that in the dislocation-free sample. It is also found that the stress caused by an In-bonded quartz-plate transducer changes the attenuation remarkably below 3 K. Therefore ZnO piezoelectric thin films were used in the present study. The observations are explained semiquantitatively in terms of the acceptor-hole–lattice interactions in the effective-mass approximation by taking the distribution of the internal stresses into account after Suzuki and Mikoshiba. The apparent difference in the contributions to the attenuation from the correlation among the impurities and from the dislocations is ascribed to the differences in the distribution of the internal stresses. It is pointed out that the degeneracy of the acceptor ground state is lifted even in the samples with boron content of 5×10^{16} cm^{-3} because of the electronic correlations among the randomly distributed impurities.

I. INTRODUCTION

Ultrasonic attenuation at low temperatures in *lightly or heavily* doped n-type Si is well explained in terms of the relaxation process of electrons among donor levels or among valleys of the conduction band.[1–7] The change in the elastic modulus in *heavily doped* p-type Si is also explained in terms of the coupling between acoustic waves and degenerate hole gas.[8]

Recently, Suzuki and Mikoshiba[9] proposed a model to explain the ultrasonic attenuation in *lightly doped* p-Si,[1] in which holes are bound to acceptors at low temperatures. The model is based on the following terms: (a) The coupling between holes and acoustic waves is calculated in the regime of the effective-mass approximation by using the acceptor-hole-lattice coupling Hamiltonian[10] and by assuming that the wave functions of the relevant acceptor states are representable by s-like envelope functions. (b) The presence of randomly distributed internal stresses is assumed, which split the fourfold ground levels of the acceptors into Kramers' doublets.[11] To take the internal stresses into the theory in a tractable way, the random local stresses are represented by the nor-